Protein Science (1999), *8*:2663–2671. Cambridge University Press. Printed in the USA.

Structure of the fibrinogen γ-chain integrin binding and factor XIIIa cross-linking sites obtained through carrier protein driven crystallization

SCOTT WARE,[1] JOHN P. DONAHUE,[2,3] JACEK HAWIGER,[2] AND WAYNE F. ANDERSON[1]

[1]Department of Molecular Pharmacology and Biological Chemistry, Northwestern University Medical School, 303 East Chicago Avenue, Chicago, Illinois 60611
[2]Department of Microbiology and Immunology, Vanderbilt University School of Medicine, Nashville, Tennessee 37232

(RECEIVED July 27, 1999; ACCEPTED October 6, 1999)

Abstract

The human fibrinogen γ-chain C-terminal segment functions as the platelet integrin binding site as well as the Factor XIIIa cross-linking substrate and thus plays an important role in blood clot formation and stabilization. The three-dimensional structure of this segment has been determined using carrier protein driven crystallization. The C-terminal segment, γ-(398–411), was attached to a linker sequence at the C-terminus of glutathione S-transferase and the structure of this fusion protein determined at 1.8 Å resolution. Functional studies of the chimeric protein demonstrate that the fibrinogen sequence in the presence of the carrier protein retains its specific functions as ligand for platelet integrin $\alpha_{IIb}\beta_3$ (gpIIb/IIIa) and as a cross-linking substrate for Factor XIIIa. The structure obtained for the fibrinogen γ-chain segment is not affected by crystal packing and can provide the missing links to the recently reported model of cross-linked fibrin.

Keywords: crystallization; crystal structure; fibrinogen; fusion protein; glutathione S-transferase; integrin

The binding of human fibrinogen to the integrin $\alpha_{IIb}\beta_3$ (glycoproteins gpIIb/IIIa) receptor on activated platelets underlies their aggregation that is responsible for physiological hemostasis and for pathological vaso-occlusive thrombi, a major trigger of heart attacks and strokes. The structure of human fibrinogen (M_r 340,000) is complex, being composed of three pairs of nonidentical polypeptide chains (α, β, and γ), which are extensively linked by disulfide bonds to form an elongated dimeric molecule (for review, see Hawiger, 1995; Doolittle et al., 1996). The segment of fibrinogen responsible for binding to the platelet $\alpha_{IIb}\beta_3$ integrin and aggregation of activated platelets has been mapped to the C-terminal region of the γ-chain and pinpointed to the continuous 12-amino acid sequence encompassing residues 400–411. This segment is both necessary and sufficient for optimal reactivity with platelet $\alpha_{IIb}\beta_3$ (Kloczewiak et al., 1984; Peerschke et al., 1986; Kloczewiak et al., 1989; Farrell et al., 1992). The second important function of the C-terminal segment of the γ-chain is related to its role in the stabilization of fibrin. Following thrombin-catalyzed conversion of soluble plasma fibrinogen into insoluble fibrin, thrombin-activated Factor XIIIa enzymatically cross-links Lys406 and Glu398 or Glu399 on opposing C-terminal segments of the γ-chain (Chen & Doolittle, 1971; Purves et al., 1987). The fibrinogen γ-(397–411) segment also serves as the ligand for the clumping receptor on pathogenic staphylococci (Strong et al., 1982).

Until recently, there was a paucity of structural information concerning functional segments of human fibrinogen. Two-dimensional NMR analysis of free fibrinogen γ-(400–411) peptide in solution indicated the presence of a type II β-turn spanning residues Gln407 to Asp410 (Blumenstein et al., 1992). Analysis of transfer nuclear Overhauser effect (NOE) measurements suggested that when bound to the integrin $\alpha_{IIb}\beta_3$ the γ-(400–411) peptide had one or two turns of helix centered around residue 406 (Mayo et al., 1996). Subsequently Teller and colleagues (Yee et al., 1997) and Doolittle and colleagues (Spraggon et al., 1997) reported the three-dimensional structures of a 30 kD fragment of human fibrinogen γ-chain and the 80 kD fragment D of human fibrinogen, respectively. However, neither study provided information on the structure of the complete γ-(398–411) segment of the γ-chain. We have developed a method, carrier protein-driven crystallization, for crystallizing small functional protein segments so that their three-dimensional structures can be determined by X-ray diffraction analysis. Using chicken egg white (CEW) lysozyme as the carrier protein, we earlier obtained crystals of the fibrinogen γ-chain C-terminal segment linked to the C-terminus of CEW lysozyme and deter-

Reprint requests to: Wayne F. Anderson, Department of Molecular Pharmacology and Biological Chemistry, Drug Discovery Program, Northwestern University Medical School, 303 East Chicago Avenue, Chicago, Illinois 60611; e-mail: wf-anderson@nwu.edu.

[3]Present address: Department of Medicine, Division of Infectious Diseases, Vanderbilt University School of Medicine, Nashville, Tennessee 37232.

mined the structure of the fibrinogen γ-chain segment (Donahue et al., 1994). The observed structure was generally extended with two wide turns.

The protein segments that are investigated using the carrier protein-driven crystallization technique are not expected to be part of a stable protein core. Rather, they would be expected to interact very weakly with the carrier protein surface. Consequently, it is possible that the observed structure could be affected by crystal packing interactions. Due to the concern that the earlier structure of the γ-chain segment 398–411 using lysozyme as the carrier protein could be influenced by crystal packing interactions, we have utilized carrier protein-driven crystallization with *Schistosoma japonicum* glutathione S-transferase (GST) as the carrier in lieu of CEW lysozyme. This allows an examination of the structure of the fibrinogen γ-chain segment in a completely different crystalline environment. The resulting chimeric protein containing the γ-(398–411) segment attached to a linker sequence at the C-terminus of GST was fully functional in terms of its binding to integrin $\alpha_{IIb}\beta_3$ and cross-linking by activated Factor XIII. The crystal structure of the fibrinogen γ-chain C-terminal segment fused to GST has been determined and eliminates the concern that crystal packing interactions affect the observed structure. Furthermore, comparison with the previously obtained structure fused to CEW lysozyme reveals a similar shape, indicating the general utility of this approach to the structural analysis of difficult-to-crystallize proteins or protein fragments.

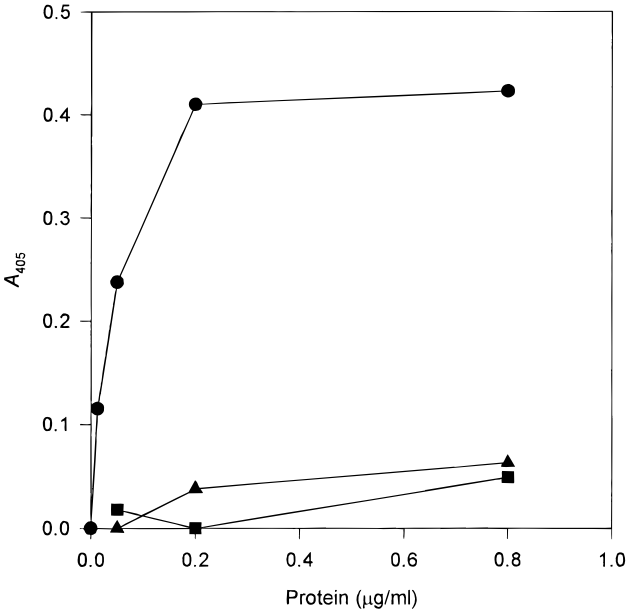

Fig. 1. Binding of the GST-fibrinogen γ-(398–411) fusion protein to platelet integrin $\alpha_{IIb}\beta_3$ determined by an ELISA system. The assay was done as described in the text, and the average of triplicate determinations is shown. ●, GST-fibrinogen γ-(398–411) with $\alpha_{IIb}\beta_3$; ▲, GST-fibrinogen γ-(398–411) without $\alpha_{IIb}\beta_3$; ■, GST with $\alpha_{IIb}\beta_3$.

Results and discussion

Functional characterization of GST-fibrinogen γ-(398–411)

To assess whether the γ-chain sequence present as a C-terminal extension of GST could adopt a biologically active conformation, we measured the integrin $\alpha_{IIb}\beta_3$ binding activity and Factor XIIIa-catalyzed cross-linking. As shown in Figure 1, binding of GST-fibrinogen γ-(398–411) to immobilized integrin $\alpha_{IIb}\beta_3$ was concentration dependent and saturable at 0.2 μg mL^{-1} of protein. This binding was dependent on the presence of the fibrinogen γ-(398–411) and of the $\alpha_{IIb}\beta_3$ receptor as shown by appropriate controls. In a reaction catalyzed by the human transglutaminase, Factor XIIIa, GST-fibrinogen γ-(398–411) monomers were cross-linked (Fig. 2). Both GST-fibrinogen γ-(398–411) dimers and tetramers were detected in this reaction, but the dimeric form was predominant. In control reactions, Factor XIIIa-catalyzed cross-linking of wild-type GST was not detected, demonstrating the specificity of the reaction for the γ-(398–411) sequence.

These functional tests reveal that the fibrinogen γ-(398–411) segment attached to GST is active as a ligand in binding to the $\alpha_{IIb}\beta_3$ integrin receptor and as a substrate for Factor XIIIa cross-linking. Thus, the carrier protein does not prevent the fibrinogen γ-(398–411) segment from adopting its biologically functional conformation, and the fusion protein structure is relevant to understanding the relationship between structure and function for this biologically important sequence.

Structure of GST-fibrinogen γ-(398–411)

The uncertainty whether the crystal environment and packing interactions may affect the structure of the fusion peptide was addressed by refinement of the two subunits independently, without noncrystallographic symmetry restraints. The terminal eight residues of the GST, the linker peptide, and the 14 residues of the fibrinogen sequence were added to the model in stages based on density in $F_o - F_c$ difference electron density maps. The free-*R* (Brünger, 1992a) was used to discriminate between different possible models derived from alternate interpretations of the electron density. The final model is that which gave the lowest free-*R*. A simulated annealing omit map in which both linkers and fibrinogen γ-chain segments were omitted is shown in Figure 3 with the refined structure placed in the electron density. For the final model (Fig. 4), including 468 amino acid residues, two glutathione molecules, and 670 solvent molecules (4,526 total atoms), the crystallographic *R* value to 1.8 Å resolution is 18.5% and the free-*R* value is 22.6%.

Glutathione S-transferase appears to have been an excellent choice for a carrier protein. In contrast to lysozyme, the GST fusion proteins can be expressed at high levels and are easily purified. Secondly, the C-terminus is solvent accessible so no structural alterations are required. Finally, this tetragonal crystal form has a high solvent content. The V_M for this crystal form is 3.7 Å^3 Da^{-1}, which corresponds to a solvent content of ~67%. In spite of the high solvent fraction, the crystals are well ordered. The glutathione S-transferase subunit structure has not been affected by the addition of the linker peptide and the fibrinogen γ-(398–411) segment. The root-mean-square deviation (RMSD) in the α-carbon positions of the GST fused to the fibrinogen γ-chain segment with that of the GST structure used in the molecular replacement calculations is 0.54 Å for subunit A of the fusion protein and 0.57 Å for subunit B while the RMSD between the crystallographically independent A and B subunits is 0.43 Å. Thus, the GST carrier protein is not structurally altered by the presence of the fibrinogen γ-(398–411) segment.

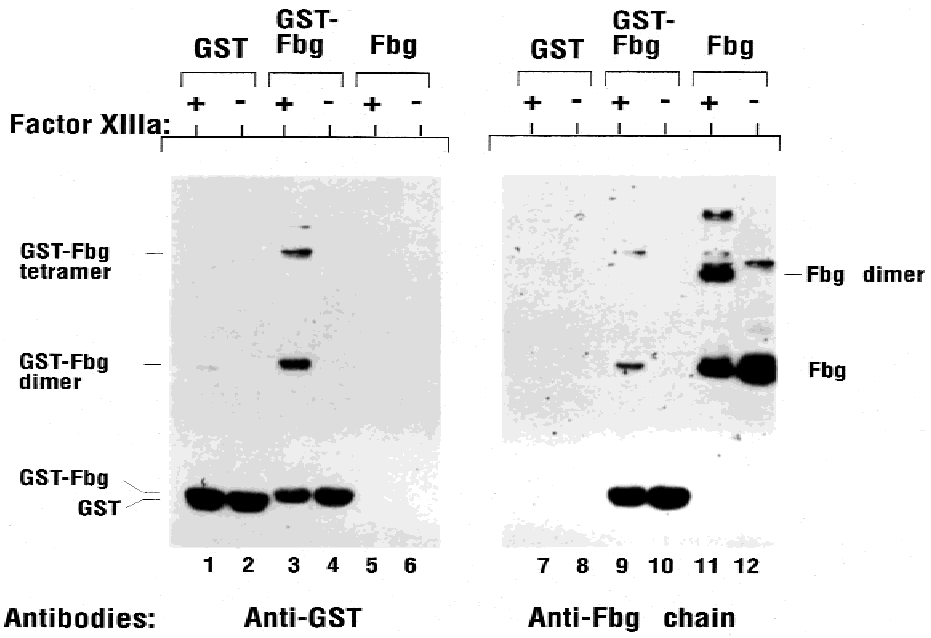

Fig. 2. Western blot analysis of Factor XIIIa cross-linking of GST-fibrinogen γ-(398–411) fusion proteins. Factor XIII cross-linking reactions were performed as described in the text.

The structure of the GST-fibrinogen γ-(398–411) fusion protein reported here is consistent with a high level of flexibility. The high temperature factors of the γ-(398–411) segment (Fig. 4) indicate that it undergoes considerably more motion than the GST carrier. The crystallographic temperature factors for the fibrinogen segment are around 80. If this were due to isotropic, harmonic motion, it would correspond to an RMS displacement of >1.0 Å around the average positions, suggesting that the C-terminus is very flexible. Indeed, since this sequence must bind to the platelet integrin $\alpha_{IIb}\beta_3$ and serve as a substrate for Factor XIIIa to produce cross-linked fibrin, a level of intrinsic flexibility would seem essential.

The γ-chain C-terminal segment also appears to exhibit conformational flexibility in the 30 kD fragment of the human fibrinogen γ-chain (Yee et al., 1997) and the 80 kD fragment D of human fibrinogen (Spraggon et al., 1997). For these crystal structures, the flexibility is sufficient to prevent crystallographic characterization of the C-terminal structure. The lack of a well-defined average structure in these cases demonstrates that the structure of the fibrinogen γ-chain segment is not determined by its interactions with the rest of fibrinogen.

The role of crystal packing and interactions with the carrier protein

The carrier protein driven crystallization approach to the determination of the fibrinogen γ-(398–411) segment places a potentially flexible structure in a new environment where it does not have strong interactions with other parts of the polypeptide chain. Although crystal packing interactions are weak and generally have only very local effects on protein structure, it is important to address the possibility that crystal packing interactions could alter the conformation of the fibrinogen γ-chain segment. Because the two subunits are crystallographically independent, they are in different

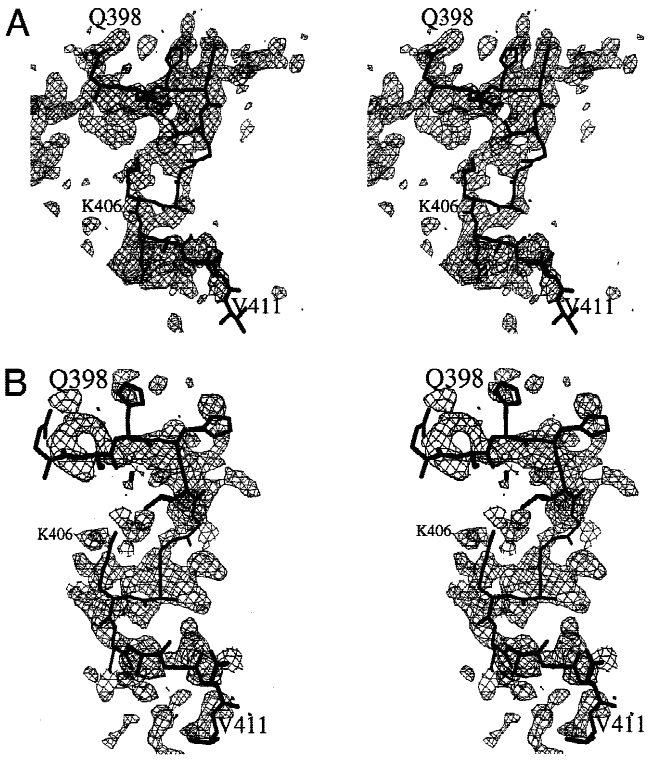

Fig. 3. A simulated annealing omit map of the two fibrinogen γ-chain segments (and the linker sequences). **A:** The γ-chain segment attached to subunit A of the GST dimer. The $F_o - F_c$ difference electron density is contoured at 2.2 times the RMS electron density of the map. **B:** The γ-chain segment attached to subunit B of the GST dimer. The weaker $F_o - F_c$ difference electron density for this subunit is contoured at 1.8 times the RMS electron density of the map. The figure was prepared using the Program O (Jones & Kjeldgaard, 1995)

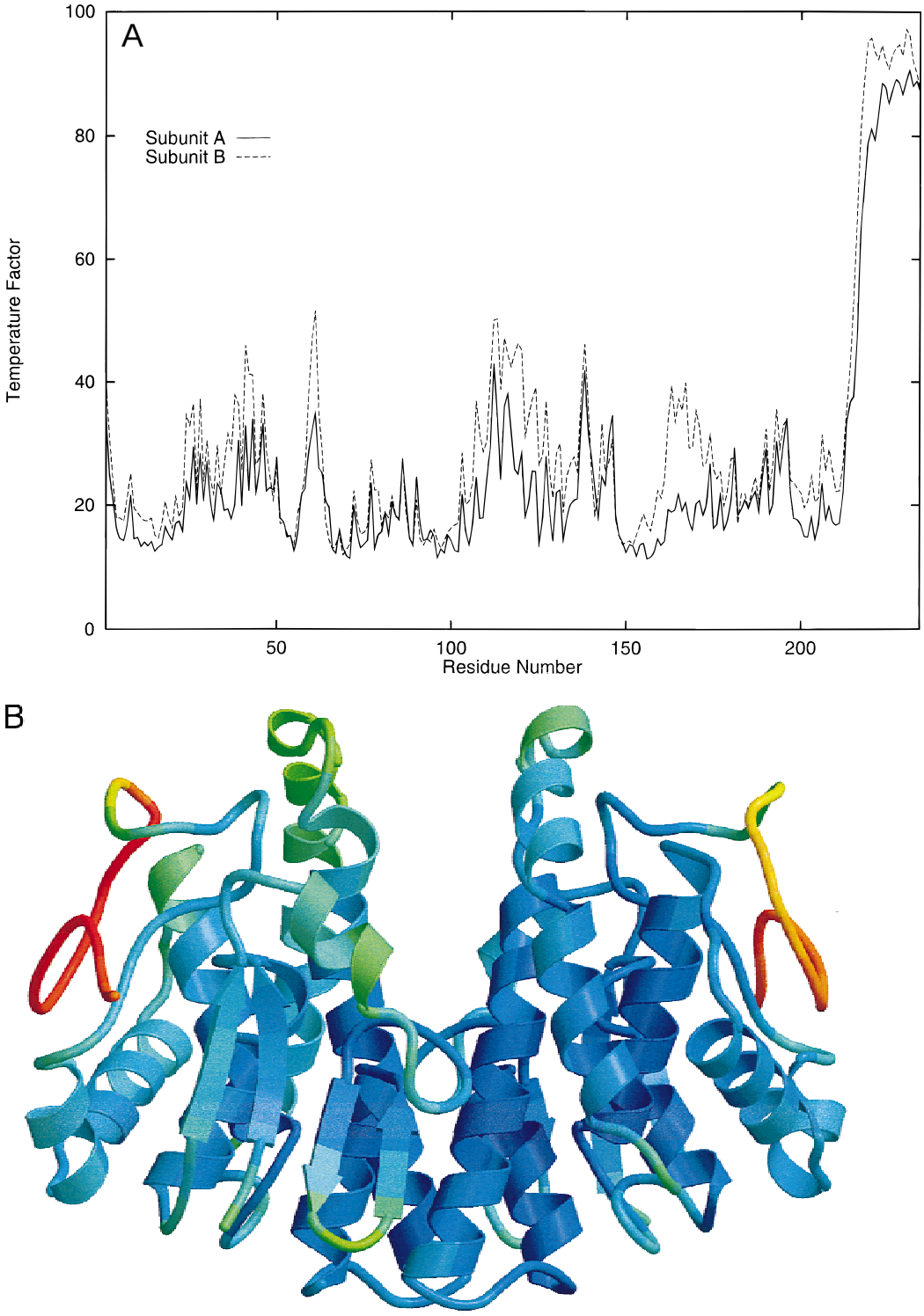

Fig. 4. A: The crystallographic temperature factors averaged for each residue. **B:** Ribbon drawing of the GST-fibrinogen γ-(398–411) dimer colored to represent the variation of temperature factor with sequence. The color scale goes from B = 0, violet to B = 100, red. The C-terminal extension comprised of the linker sequence and the fibrinogen γ-chain segment lies on the surface away from the dimer interface.

crystal environments and potentially could have different crystal packing interactions. Comparison of the fibrinogen γ-(398–411) segment from the two crystallographically independent GST subunits (Fig. 5A) gives an RMSD of 1.54 Å for all atoms and 1.07 Å for the α-carbons of this segment. The deviation for the γ-(398–411) segment is 2.2 Å for G403. This RMSD is consistent with that

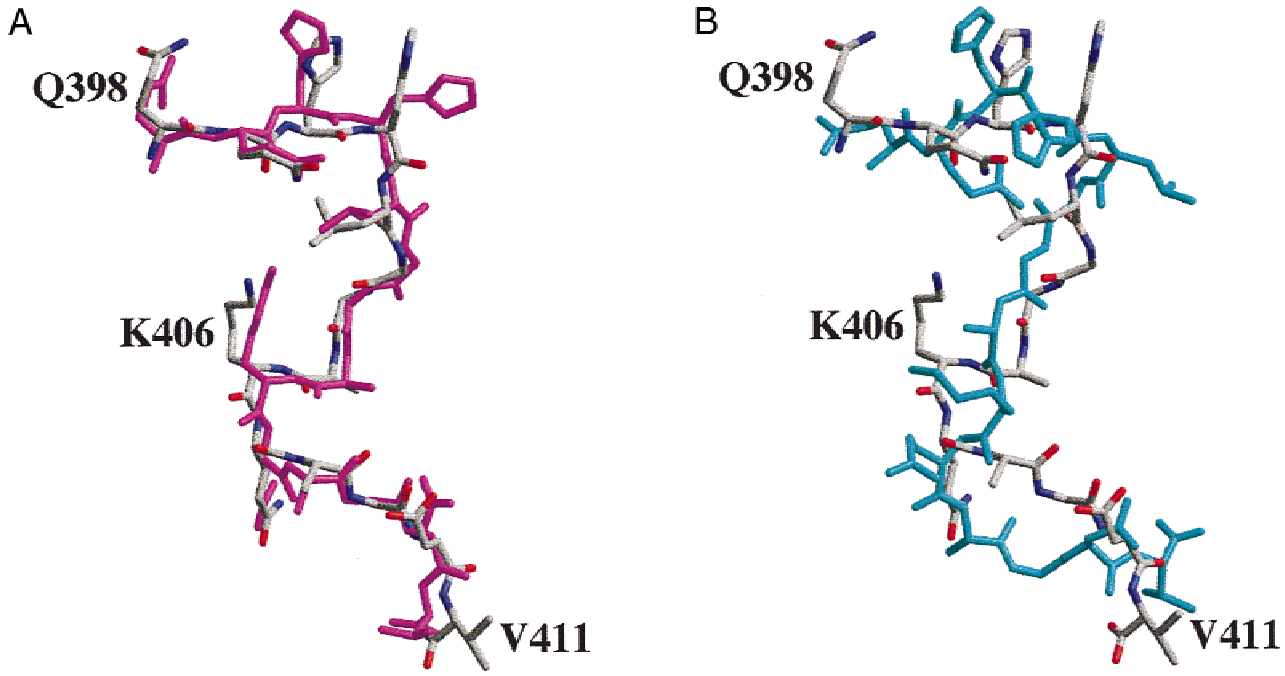

Fig. 5. A: Comparison of the fibrinogen γ-(398–411) segment attached to GST subunits A and B. The atoms of subunit A have carbons colored grey, oxygens red, and nitrogens blue, while subunit B is all magenta. The γ-chain segments are superimposed by their alpha carbons (1.07 Å RMSD). **B:** Comparison of the fibrinogen γ-(398–411) segments attached to GST subunit A (colored as in **A**) and CEW lysozyme (colored cyan) illustrating the common Z shape. This figure was made using the program Raster3D (Bacon & Anderson, 1988; Merritt & Murphy, 1994).

expected for residues with an average crystallographic temperature factor, or B, of >80. Superimposing the crystallographically independent A and B subunits of GST-fibrinogen γ-(398–411) reveals that the largest differences are in the most poorly defined regions, particularly the linker sequence (residues 217–220) connecting GST with fibrinogen γ-chain residues 398–411, which have deviations of 1.3 to 6.1 Å. Neither fibrinogen γ-chain segment makes any direct interactions with neighboring molecules in the crystal lattice.

The lack of crystal packing interactions involving the fibrinogen γ-(398–411) segment is also reflected in its higher crystallographic temperature factors in the crystal lattice of the GST fusion compared to the more tightly packed lysozyme fusion where the average *B* for the fibrinogen γ-(398–411) segment was 33. Thus, crystal packing interactions can be ruled out as a significant concern.

The observed structures, however, could be affected by the presence of the carrier protein. As in the case of the lysozyme fusion, there are few interactions of the fibrinogen γ-(398–411) segment with the carrier protein. The interactions between the fibrinogen γ-(398–411) segment and the GST carrier are not extensive. There is a total of only 485 $Å^2$ of surface area buried between the fibrinogen segment (273 $Å^2$) and the GST carrier (212 $Å^2$). Moreover, the largest contributions to the buried surface come from hydrophilic residues, Gln398, Lys406, Gln399, and His401. There are also few hydrogen bonds between the fibrinogen segment and the GST carrier. Only two occur in both of the crystallographically independent molecules. The Gln399 side-chain hydrogen bonds to the hydroxyl of Tyr155 of GST, and the main-chain carbonyl oxygen of Ala405 hydrogen bonds to the main-chain amide nitrogen of Ala199. The additional two or five hydrogen bonds between the fibrinogen segment and the GST differ between the two subunits and are primarily between flexible, polar side chains. These interactions would not be expected to contribute greatly to defining the structure of the fibrinogen segment. Similarly, there are many (13 and 11 for molecules A and B, respectively) hydrogen bonds to ordered water molecules that would not be expected to alter the structure of the fibrinogen segment. The results thus suggest that GST has little effect on the structure of the fusion peptide. These few interactions are unlikely to provide sufficient energy to drive the structure into a significantly less favorable conformation. The lack of strongly stabilizing interactions with the GST carrier is also indicated by the high temperature factors observed for the fibrinogen γ-chain segment.

Comparison with other fibrinogen γ-(398–411) structures

At the time the structure of the lysozyme fibrinogen γ-(398–411) fusion protein was determined, the only other information on the structure of the fibrinogen γ-(398–411) segment available was from NMR studies of synthetic peptides. Since that time, the structures that have been reported for the fibrinogen γ-chain C-terminal 30 kD fragment (Yee et al., 1997), the fibrinogen fragment D, and the cross-linked fragment D (or double D) (Spraggon et al., 1997) should have provided the structure of the fibrinogen γ-(398–411) segment as part of the fibrinogen molecule. Unfortunately, in all of these recent structures, much of the fibrinogen γ-(398–411) segment is either missing due to proteolysis or appears to be disordered. The only information that is available is for residues 398–403 (Yee et al., 1997). The few residues observed in the γ-chain 30 kD fragment and the high temperature factors of the γ-(398–411)

residues in the GST fusion protein make a detailed comparison difficult. Nevertheless, comparison of the conformation of these few residues with that present in the two fusion proteins (lysozyme and GST) bearing a fibrinogen γ-chain segment reveals a general similarity for residues 398–401. This segment adopts an extended structure in each case. Comparing the peptide backbone atoms of residues γ-398–401 in the GST fusion (subunit A) and the 30 kD fragment of the fibrinogen γ-chain (Protein Data Bank (PDB) entry 1FID) (Yee et al., 1997) gives an RMSD of 1.09 Å. In the three examples for the 30 kD fragment of the fibrinogen γ-chain, residues 402 and 403 continue this extended region while in both of the fusion proteins there is a bend at His401 and Leu402.

Comparison of the fibrinogen γ-chain segment structure in the very different contexts provided by crystallization of the GST and lysozyme carrier proteins reveals an overall similarity in its shape (Fig. 5B). The shape similarity occurs despite the lack of interactions between residues separated in the sequence and despite the different environments of the γ-chain segments. Superimposing the fibrinogen γ-chain segments from the GST fusion protein and the CEW lysozyme fusion protein reveal that the carrier proteins lay on opposite sides of the fibrinogen segment. Although the conformational angles differ, the Gln398GlnHisHis401 section is extended in all six examples of the fibrinogen γ-chain segment in which it is observed. The Leu402GlyGlyAla405 section is only observed in the examples provided by carrier protein driven crystallization, where it is extended in each case. The largest structural differences are seen at two sites that appear to be the most sensitive to their environment. They occur around the His401–Leu402 sequence and in the Lys406, Gln407 region. Thus, it is somewhat surprising that the fibrinogen γ-(398–411) segment has a very similar overall Z-like shape in the GST and CEW fusion proteins despite the different crystalline environments and that the carrier proteins are on opposite sides of the Z shaped γ-chain segment. The structural differences observed in the two fusion proteins analyzed by us are likely to represent easily accessible conformational states of the fibrinogen γ-(398–411) segment, and the structural similarities to represent preferred conformations.

The results demonstrate that crystal packing interactions have not affected the structure of the fibrinogen segment, and that the fibrinogen γ-(398–411) segment retains bioactivity when attached to the GST carrier protein. Furthermore, GST fusion proteins with different sequences attached at the C-termini have different structures (Lim et al., 1994; McTigue et al., 1995; Rossjohn et al., 1998); therefore, it seems reasonable that the structure observed for the fibrinogen γ-(398–411) segment is determined primarily by its own amino acid sequence. However, while the γ-chain segments maintain the identifiable Z shape (see Fig. 5B), there are discernible differences in the structures of the fibrinogen γ-(398–411) segments in the context of the lysozyme and GST fusions. The largest deviations (3.7–5.0 Å) occur in the two residues preceding or following residue 407. These are regions that could be affected by crystal packing interactions in the more tightly packed lysozyme-γ-(398–411) fusion protein crystals.

Model of cross-linked γ-(398–411)

Based on the spacing of the glutamine and lysine residues cross-linked by activated Factor XIII, it was proposed that the fibrinogen γ-chain C-terminal segment may be helical, since both residues would then be on the same side of the helix (Doolittle, 1973). However, neither a helical conformation nor a fully extended conformation is consistent with the 16.4 Å distance between the last observed residues (Gln398 in one subunit and Glu396 in the other subunit) of the cross-linked fragment D crystal structure (Spraggon et al., 1997).

To determine if the observed structure of the fibrinogen γ-(398–411) segment was compatible with the structure of the cross-linked fibrin fragment D, an approximate model of the cross-linked γ-(398–411) segment was constructed. The question being addressed is simply whether the γ-(398–411) structure can be placed on the cross-linked Fragment D structure, completing that structure, and be positioned such that it would allow cross-links between the side chains of Gln398 of one molecule and Lys406 of the second. Perhaps surprisingly, by allowing the side chain conformations of Gln398 and Lys406 to vary, this can be done while minimizing steric clashes between the two γ-(398–411) segments. Furthermore, the γ-(398–411) segments provide a bridge between the two fibrin molecules (Fig. 6) without any steric interference that would require changes in the fragment D structure. This approximate model suggests that the C-terminal segments would be in a very exposed location where they could interact with the platelet $\alpha_{IIb}\beta_3$ integrin receptor or be cross-linked by Factor XIIIa. Thus, even though the fibrinogen γ-(398–411) structure was determined in an uncross-linked state as part of a GST fusion protein, it is consistent with the available structural data for cross-linked fibrin.

Taken together, our data indicate that the crystal structures of the C-terminal segment of the γ-chain of human fibrinogen have similarities despite the different crystal environments and different carrier proteins used. It provides much needed structural information about a functionally important part of fibrinogen hitherto not available from conventional crystallization approaches.

Materials and methods

Construction of the GST-fibrinogen γ-(398-411) expression plasmid

The following complementary oligonucleotides encoding the 14 C-terminal residues of the fibrinogen γ-chain (Chung et al., 1983) were synthesized:

```
GAT CCA CAG CAA CAC CAC CTA GGG GGA GCC AAA CAG GCT GGA GAC GTT TAA G
     GT GTC GTT GTG GTG GAT CCC CCT CGG TTT GTC CGA CCT CTG CAA ATT CTTAA
        gln gln his his leu gly gly ala lys gln ala gly asp val ***
```

After annealing, the resulting double stranded oligonucleotide contained a translation termination codon immediately following Val411 and *Bam*HI and *Eco*RI sticky ends at 5′ and 3′ termini. This DNA fragment was ligated into *Bam*HI/*Eco*RI digested pGEX-1 (Smith & Johnson, 1988) to produce an in-frame fusion with the C-terminus of *S. japonicum* glutathione S-transferase.

GST-fibrinogen γ-(398-411) expression, purification, and crystallization

The GST-fibrinogen γ-(398–411) chimeric protein was expressed in *Escherichia coli* strain DH5α and then purified using glutathione-agarose affinity chromatography essentially as described (Smith & Johnson, 1988).

The GST-fibrinogen γ-(398–411) fusion protein was crystallized by the hanging drop vapor diffusion method using PEG as the precipitant. A 4 μL drop containing ~20 μg of protein (2 μL of a

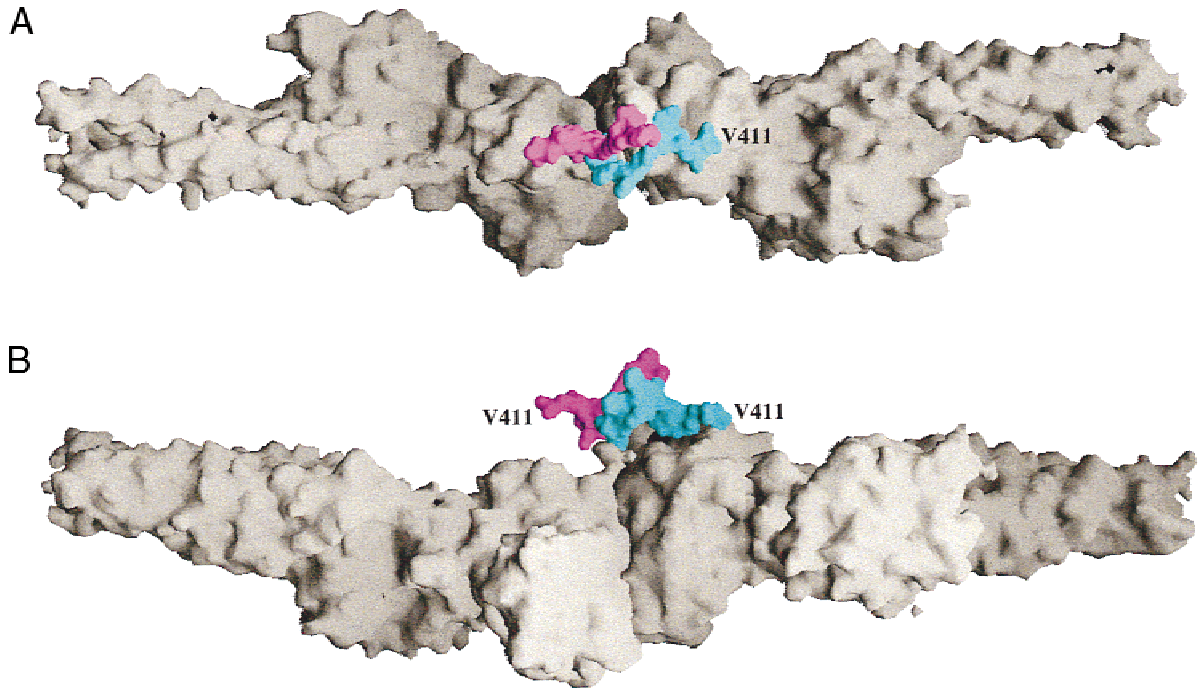

Fig. 6. Model of cross-linked fibrinogen fragment D constructed from two GST-fibrinogen γ-(398–411) segments (colored cyan and magenta) positioned at the C-termini of the γ-chains of the cross-linked fibrin fragment D structure (colored gray, PDB entry 1FZB) so that the Glu398 and Lys406 side chains could form cross-links. **A:** View looking down the pseudo-twofold where the end-to-end interactions between fibrin molecules occur. The long axis of the fibrin molecules is horizontal. **B:** View rotated 90° from that in **A**. The pseudo-twofold is vertical. This picture was made with the program GRASP (Nicholls et al., 1993).

10 mg/mL protein solution), 8% PEG 3350, 50 mM sodium acetate pH 4.6, 25 mM sodium chloride, 17.5 mM ammonium sulfate, 5 mM Tris and 5 mM reduced glutathione was equilibrated with a 1.0 mL reservoir of 16% PEG 3350, 100 mM sodium acetate pH 4.6 and 35 mM ammonium sulfate. The crystals obtained were space group $P4_12_12$ with cell dimensions at −170 °C of $a = b =$ 105.8 Å, c = 137.2 Å. X-ray diffraction data was collected on beamline X4A at the National Synchrotron Light Source at Brookhaven National Laboratory using a wavelength of 1.0093 Å. The image plate data were integrated with DENZO and scaled with SCALEPACK (Otwinowski & Minor, 1997). The data collection statistics are presented in Table 1.

GST-fibrinogen γ-(398–411) structure determination

The structure of the GST-fibrinogen γ-(398–411) chimeric protein was determined using the molecular replacement method (Rossmann, 1990). The starting model was taken from residues 1–209 of entry 1GNE (Lim et al., 1994) in the Brookhaven PDB (Bernstein et al., 1977). The program AMoRe (Navaza, 1994) was used to determine rotation and translation parameters. Inspection of those parameters revealed that the correct space group was $P4_12_12$ and that the asymmetric unit was a dimer containing two complete GST subunits. The initial dimer model was created by applying the rotation and translation parameters determined by AMoRe to the starting model. This model was subjected to rigid body refinement in X-PLOR (Brünger, 1992b), which yielded an *R*-factor of 35.8% and a free *R*-factor (Brünger, 1992a) of 38.2%. A cycle of simulated annealing refinement (Brünger et al., 1987, 1990) with a starting temperature of 3,000 K followed by refinement of individual *B*-factors was then performed using X-PLOR, which yielded an *R*-factor of 29.3% and a free *R*-factor of 34.0%. After this initial refinement, inspection of an $F_o - F_c$ electron density map (Read, 1986; Kleywegt & Brünger, 1996) indicated some portions of the fibrinogen γ-(398–411) segment, but not the complete linker or fibrinogen sequence.

Table 1. *Data collection and refinement statistics*

Data collection			
Resolution limits	28–1.7 Å		
Total reflections	376,772		
Unique reflections	67,736		
Completeness	89.2% (66.1%, 2.0–1.8 Å)		
R_{merge}	5.4%		
Molecular replacement			
Resolution range	8–4 Å		
Rotation angles (deg)	37.65	110.18	54.53
Translation (fractional)	0.1368	0.4326	0.1122
Refinement			
Resolution	28–1.8 Å		
Reflections used	57,456		
R	18.5%		
R_{free}	22.6%		
RMSD bond lengths	0.007 Å		
RMSD bond angles	1.425°		

After the partially refined model was subjected to several subsequent refinement cycles including simulated annealing with torsion angle dynamics (Rice & Brünger, 1994) and the addition of ordered water molecules, the quality of the electron density maps improved considerably and a polyalanine model consisting of the entire γ-(398–411) segment was fit to density visible in $F_o - F_c$ maps in subunit A. The density visible near the C-terminal region of subunit B was not as easily interpretable, and gaps corresponding to residues B218–B222 and B226–B228 were left in the model. After further refinement, the quality of the model was further improved by rebuilding based on simulated annealing omit maps (Hodel et al., 1992), the addition of side chains to the polyalanine segments, addition of ordered water molecules, and the use of a bulk solvent correction (Jiang & Brünger, 1994). The final model, which contains 468 residues, two glutathione molecules, and 670 water molecules, has an *R*-factor of 18.5% and a free *R*-factor of 22.6%. Eighty-seven percent of the residues fall within the most favorable regions of a Ramachandran plot, and none are within the disallowed regions.

Measurement of binding of GST-fibrinogen γ-(398–411) to platelet integrin $\alpha_{IIb}\beta_3$

The platelet fibrinogen receptor (integrin $\alpha_{IIb}\beta_3$, 10 μg/mL) was purified from outdated human platelets as described (Phillips et al., 1992). Purified $\alpha_{IIb}\beta_3$ (10 μg/mL) in TBSC buffer (20 mM Tris-HCl, pH 7.6, 150 mM NaCl, 1 mM $CaCl_2$) was applied to the wells of Immulon 2 (Dynatech Laboratories, Inc., Shantilly, Virginia) microtiter plates. The plates were incubated for 18 h at room temperature. After adsorption of $\alpha_{IIb}\beta_3$, all wells were blocked with 1% BSA in coating buffer. After incubation for 1 h at room temperature, protein-coated wells were washed with TBSC (20 mM Tris-HCl, pH 7.6, 150 mM NaCl, 1 mM $CaCl_2$). Decreasing concentrations of GST-fibrinogen γ-(398–411) or GST, diluted with TBSC, were added. Plates were incubated for 2 h at room temperature and washed with TBSC. Polyclonal GST antibody was added to all wells, incubated for 1 h at room temperature, and washed with TBSC. Goat anti-rabbit IgG conjugated to alkaline phosphatase (Sigma Chemical Co., St. Louis, Missouri) was added to all wells, incubated for 1 h at room temperature, and washed with TBSC. A 1 mg/mL solution of *p*-nitrophenyl phosphate (Pierce, Rockford, Illinois) in 1 M Tris-HCl (pH 9.5) was added to all wells and incubated in the dark for 2 h at room temperature. Absorbance at 405 nm was determined using a Titertek Multiskan Plus microtiter plate reader.

Factor XIIIa cross-linking of GST-fibrinogen γ-(398–411)

Human plasma Factor XIII (Calbiochem, La Jolla, California) was activated with thrombin (0.5 unit; Sigma Chemical Co.) for 30 min at 37 °C. The reaction was quenched by the addition of hirudin (0.5 unit; Sigma Chemical Co.) and incubation at 37 °C for 10 min. Activated Factor XIII was added to fibrinogen, GST-fibrinogen γ-(398–411) or wild-type GST in TBS plus 2 mM $CaCl_2$ and incubated at 37 °C for 18 h. The products of the cross-linking reaction were analyzed by SDS-PAGE and Western blotting using antibodies to recombinant GST and to fibrinogen γ-chain peptide (residues 385–411).

Acknowledgments

S.W. and J.P.D. contributed equally to the completion of this work. The assistance of Caryl Gates and Ludmilla Shuvalova in the crystallization of the GST-γ-(398–411) chimeric protein and Joseph Brunzelle in the preparation of figures is gratefully acknowledged. The diffraction data were collected at the National Synchrotron Light Source, Brookhaven National Laboratory, which is supported by the U.S. Department of Energy, Division of Materials Sciences and Division of Chemical Sciences, on beamline X4A, which is supported by the Howard Hughes Medical Institute. The instruction of Craig Ogata on the use of the data collection facility is appreciated. This work was supported in part by NIH grant HL45994 (J.H.).

References

Bacon DJ, Anderson WF. 1988. A fast algorithm for rendering space-filling molecule pictures. *J Mol Graphics 6*:219–220.

Bernstein FC, Koetzle TF, Williams GJB, Meyer EF Jr, Brice MD, Rodgers JR, Kennard O, Shimanouchi T, Tasumi M. 1977. The Protein Data Bank: A computer-based archival file for macromolecular structures. *J Mol Biol 112*:535–542.

Blumenstein M, Matsueda GR, Timmons S, Hawiger J. 1992. A beta-turn is present in the 392–411 segment of the human fibrinogen gamma-chain. Effects of structural changes in this segment on affinity to antibody 4A5. *Biochemistry 31*:10692–10698.

Brünger AT. 1992a. Free *R* value: A novel statistical quantity for assessing the accuracy of crystal structures. *Nature 355*:472–475.

Brünger AT. 1992b. *X-PLOR version 3.1: A system for X-ray crystallography and NMR*. New Haven: Yale University Press.

Brünger AT, Krukowski A, Erickson J. 1990. Slow-cooling protocols for crystallographic refinement by simulated annealing. *Acta Crystallogr A46*:585–593.

Brünger AT, Kuriyan J, Karplus M. 1987. Crystallographic *R* factor refinement by molecular dynamics. *Science 235*:458–460.

Chen R, Doolittle RF. 1971. Cross-linking sites in human and bovine fibrin. *Biochemistry 10*:4487–4491.

Chung DW, Chan WY, Davie EW. 1983. Characterization of a complementary deoxyribonucleic acid coding for the gamma chain of human fibrinogen. *Biochemistry 22*:3250–3256.

Donahue JP, Patel H, Anderson WF, Hawiger J. 1994. Three-dimensional structure of the platelet integrin recognition domain of the fibrinogen γ-chain obtained by carrier protein driven crystallization. *Proc Natl Acad Sci USA 91*:12178–12182.

Doolittle RF. 1973. Structural aspects of the fibrinogen to fibrin conversion. *Adv Prot Chem 27*:1–109.

Doolittle RF, Everse SJ, Spraggon G. 1996. Human fibrinogen: Anticipating a 3-dimensional structure. *FASEB J 10*:1464–1470.

Farrell DH, Thiagarajan P, Chung DW, Davie EW. 1992. Role of fibrinogen alpha and gamma chain sites in platelet aggregation. *Proc Natl Acad Sci USA 89*:10729–10732.

Hawiger J. 1995. Adhesive ends of fibrinogen and its antiadhesive peptides: The end of a saga? *Semin Hematol 32*:99–109.

Hodel A, Kim S-H, Brünger AT. 1992. Model bias in macromolecular crystal structures. *Acta Crystallogr A48*:851–858.

Jiang J-S, Brünger AT. 1994. Protein hydration observed by X-ray diffraction: Solvation properties of penicillopepsin and neuraminidase crystal structures. *J Mol Biol 243*:100–115.

Jones TA, Kjeldgaard M. 1995. *O—The manual (version 5.10)*. Uppsala: Uppsala University. pp 1–172.

Kleywegt GJ, Brünger AT. 1996. Checking your imagination: Application of the free R value. *Structure 4*:897–904.

Kloczewiak M, Timmons S, Bednarek MA, Sakon M, Hawiger J. 1989. Platelet receptor recognition domain on the gamma chain of human fibrinogen and its synthetic peptide analogues. *Biochemistry 28*:2915–2919.

Kloczewiak M, Timmons S, Lukas TJ, Hawiger J. 1984. Platelet receptor recognition site on human fibrinogen. Synthesis and structure-function relationship of peptides corresponding to the carboxy-terminal segment of the gamma chain. *Biochemistry 23*:1767–1774.

Lim K, Ho JX, Keeling K, Gilliland GL, Ji X, Ruker F, Carter DC. 1994. Three-dimensional structure of *Schistosoma japonicum* glutathione S-transferase fused with a six-amino acid conserved neutralizing epitope of gp41 from HIV. *Protein Sci 3*:2233–2244.

Mayo KH, Fan F, Beavers MP, Eckardt A, Keane P, Hoekstra WJ, Andrade-Gordon P. 1996. Integrin receptor GPIIb/IIIa bound state conformation of the fibrinogen γ-chain C-terminal peptide 400–411: NMR and transfer NOE studies. *Biochemistry 35*:4434–4444.

McTigue MA, Williams DR, Tainer JA. 1995. Crystal structures of a schistosomal drug and vaccine target: Glutathione S-transferase from Schistosoma japonica and its complex with the leading antischistosomal drug praziquantel. *J Mol Biol 246*:21–27.

Merritt EA, Murphy MEP. 1994. Raster3D version 2.0—A program for photorealistic molecular graphics. *Acta Crystallogr D50*:869–873.

Navaza J. 1994. AMoRe: An automated package for molecular replacement. *Acta Crystallogr A50*:157–163.

Nicholls A, Bharadwaj R, Honig B. 1993. Grasp: Graphical representation and analysis of surface properties. *Biophys J 64*:A166.

Otwinowski Z, Minor W. 1997. Processing of X-ray diffraction data collected in oscillation mode. *Methods Enzymol 276*:307–326.

Peerschke EIB, Francis CW, Marder VJ. 1986. Fibrinogen binding to human platelets: Effect of gamma chain carboxyterminal structure and length. *Blood 67*:385–390.

Phillips DR, Fitzgerald L, Parise L, Steiner B. 1992. Platelet membrane glycoprotein IIb-IIIa complex: Purification, characterization and reconstitution into phospholipid vesicles. *Methods Enzymol 215*:244–263.

Purves L, Purves M, Brandt W. 1987. Cleavage of fibrin-derived D-dimer into monomers by endopeptidase from puff adder venom (*Bitis arietans*) acting at cross-linked sites of the γ-chain. *Biochemistry 26*:4640–4646.

Read RJ. 1986. Improved fourier coefficients for maps using phases from partial structures with errors. *Acta Crystallogr A52*:140–149.

Rice LM, Brünger AT. 1994. Torsion angle dynamics: Reduced variable conformational sampling enhances crystallographic structure refinement. *Proteins 19*:277–290.

Rossjohn J, McKinstry WJ, Oakley AJ, Verger D, Flanagan J, Chelvanayagam G, Tan KL, Board PG, Parker MW. 1998. Human theta class glutathione transferase: The crystal structure reveals a sulfate-binding pocket within a buried active site. *Structure 6*:309–322.

Rossmann MG. 1990. The molecular replacement method. *Acta Crystallogr A46*:73–82.

Smith DB, Johnson KS. 1988. Single-step purification of polypeptides expressed in *Escherichia coli* as fusions with glutathione S-transferase. *Gene 67*:31–40.

Spraggon G, Everse SJ, Doolittle RF. 1997. Crystal structures of fragment D from human fibrinogen and its crosslinked counterpart from fibrin. *Nature 389*:455–450.

Strong DD, Laudano AP, Hawiger J, Doolittle RF. 1982. Isolation, characterization and synthesis of peptides from human fibrinogen that block the staphylococcal clumping reaction and construction of a synthetic clumping particle. *Biochemistry 21*:1414–1420.

Yee VC, Pratt KP, Cote HC, Trong IL, Chung DW, Davie EW, Stenkamp RE, Teller DC. 1997. Crystal structure of a 30 kDa C-terminal fragment from the γ-chain of human fibrinogen. *Structure 5*:125–120.